ZIKA VIRUS INDUCES ASTROCYTE DIFFERENTIATION IN NEURAL STEM CELLS

Olivia Lossia

A journal article submitted in partial fulfillment of
the requirements for the degree of
Master of Science

Neuroscience

Central Michigan University
Mount Pleasant, MI
February 2017

ACKNOWLEDGEMENTS

I would first like to thank the members of my thesis committee, Dr. Julien Rossignol, Dr. Gary Dunbar, and Dr. Michael Conway, for providing me with the knowledge and expertise to conduct my research and the opportunity to work in such a new, exciting area of science. I would also like to thank the various students who were involved in this project including Stacy Goldthorpe, Bhairavi Srinageshwar, Maya Tree, and Robert Williams. Their participation and insight into the project was immensely helpful.

ABSTRACT

ZIKA VIRUS INDUCES ASTROCYTE DIFFERENTIATION IN NEURAL STEM CELLS

by Olivia Lossia

Zika virus (ZIKV) is a rapidly emerging flavivirus that has been associated with a number of congenital neurological manifestations. Here we show that ZIKV replicates efficiently in mouse neural stem cells (mNSCs). ZIKV infection reduced the number of neurospheres over time, which correlated with development of cytopathic effect (CPE), and a significant decrease in the number of proteins secreted into mNSC supernatants. However, long term infection of neurospheres led to selection of neurospheres that were resistant to CPE. A gene expression array of neural stem cell progenitor and differentiation markers suggested that infection reduced the number of neuronal and oligodendrocyte progenitors, while increasing the number of astrocyte progenitors and associated antiviral genes. These data provide molecular and cellular evidence that ZIKV significantly alters neural development in the vertebrate host and that astrocyte differentiation may be a protective response that limits neuropathogenesis.

TABLE OF CONTENTS

Zika virus induces astrocyte differentiation in neural stem cells

Michael J. Conway[1]*, Olivia V. Lossia[1,2,3], Maya O. Tree[1], Robert J. Williams[1], Stacy C. Goldthorpe[1], Bhairavi Srinageshwar[2,3], Gary L. Dunbar[2,3,4,5], and Julien Rossignol[1,2,3].

[1]Foundational Sciences, Central Michigan University

College of Medicine, Mt. Pleasant, MI, 48859

[2]Program in Neuroscience, Central Michigan University, Mt. Pleasant, MI 48859

[3]Field Neurosciences Laboratory for Restorative Neurology,

Central Michigan University, Mt. Pleasant, MI 48859

[4]Department of Psychology, Central Michigan University, Mt. Pleasant, MI 48859

[5]St. Mary's of Michigan Field Neuroscience Institute, Saginaw, MI 48604

Address correspondence to: Foundational Sciences, Central Michigan University

College of Medicine, Mount Pleasant, MI, 48859

E-mail: michael.conway@cmich.edu. Phone: (989) 774-3930, Fax: (989) 774-3462

Running title: Zika neuropathology

Word count: 2,309

Abstract

Zika virus (ZIKV) is a rapidly emerging flavivirus that has been associated with a number of congenital neurological manifestations. Here we show that ZIKV replicates efficiently in mouse neural stem cells (mNSCs). ZIKV infection reduced the number of neurospheres over time, which correlated with development of cytopathic effect (CPE), and a significant decrease in the number of proteins secreted into mNSC supernatants. However, long term infection of neurospheres led to selection of neurospheres that were resistant to CPE. A gene expression array of neural stem cell progenitor and differentiation markers suggested that infection reduced the number of neuronal and oligodendrocyte progenitors, while increasing the number of astrocyte progenitors and associated antiviral genes.. These data provide molecular and cellular evidence that ZIKV significantly alters neural development in the vertebrate host and that astrocyte differentiation may be a protective response that limits neuropathogenesis.

Keywords: Flavivirus, Zika virus, Neuropathogenesis, Neural Stem Cell, Neural Progenitor, Astrocyte, Neuron, Differentiation

Introduction

Zika virus (ZIKV) is a rapidly emerging flavivirus that is currently spreading throughout the Western hemisphere. ZIKV is spread primarily by the mosquito vector, *Aedes aegypti*, but can also be transmitted by *Ae. albopictus*, which is more widely distributed throughout the United States (Grard et al., 2014; Wong et al., 2013). ZIKV infections are typically asymptomatic, and clinically recognized infections are characterized by mild headache, maculopapular rash, fever, malaise, conjunctivitis, and joint pain (Fauci and Morens, 2016). Presently, no targeted therapeutics or prophylactic drugs have been developed for ZIKV.

The current ZIKV outbreak in the Western hemisphere has been associated with an increase in the rate of babies born with microcephaly and other congenital neurological disorders. Rubella virus and cytomegalovirus infection are also well known causes of congenital microcephaly (Belzile et al., 2014; Kosugi et al., 1998; Li et al., 2015; Tsutsui et al., 2008). It is currently unknown how ZIKV contributes to the increased rates of microcephaly and other congenital neurological defects, although prior research suggests that ZIKV can replicate in mouse astroglial cells and neurons, and ZIKV RNA has been detected in human placental and neural tissue (Bell et al., 1971; Calvet et al., 2016; Martines et al., 2016). Recent work also suggests that ZIKV can infect human neural progenitors and mature neurons and increase expression of a marker of apoptosis. ZIKV infection can also reduce the growth of neural stem cells and brain organoids (Garcez et al., 2016; Tang et al., 2016).

Development of a mouse model of congenital ZIKV syndrome is a critical step to develop interventions that can be employed to prevent neuropathogenesis (Aliota et al., 2016;

Dowall et al., 2016; Lazear et al., 2016). Here we assess the ability of ZIKV to replicate in mouse neural stem cells (mNSC), the impact of infection on the secretory proteome (i.e., secretome) and differentiation of neural cell types.. Briefly, we found that the African lineage of ZIKV can replicate efficiently in mNSCs. Infection reduced the number of neurospheres and led to cytopathic effect (CPE). Additionally, liquid chromatography tandem mass spectrometry (LC+MS/MS) identified significant alterations in the mNSC secretome during ZIKV infection. Infection led to a decrease in the number of proteins detected 1 and 7 days post-infection (dpi). Interestingly, long-term infection led to the selection of neurospheres that were resistant to CPE. Infection significantly downregulated the gene expression of a number of genes associated with neural stem cells, neuronal cell types, and oligodendrocytes, while upregulating genes associated with astrocyte differentiation and antiviral genes such as Toll-like receptor 3 (TLR3), viperin, and CCL2.. These data suggest that ZIKV targets multiple neural cell types and induces differentiation of astrocytes and TLR3 to mitigate the cytopathology induced by ZIKV.

Results

Infection of mNSCs with Zika virus strain IB H 30656.

Previous literature suggests that ZIKV can replicate in wild-type mouse astroglial cells and neurons and lead to paralysis and death (Aliota et al., 2016; Bell et al., 1971; Dowall et al., 2016; Lazear et al., 2016; Rossi et al., 2016). To determine if mouse neural stem cells (mNSCs) are permissive to ZIKV infection, we inoculated mNSCs with approximately 5 x 10^4 genomic equivalents of ZIKV (IB H strain), unbound virus was removed, and then fresh media was added to each infection. Relative viral RNA (vRNA) was then assessed in cell-free supernatants at a zero time point, which was at the time fresh media was added, and 1, 3, 5, and 7 dpi. ZIKV

vRNA steadily increased in cell supernatants with a 1,000-fold increase 5 dpi (Fig. 1). ZIKV infection also significantly reduced the number of neurospheres in each well, and led to morphological changes that appeared like disaggregating neurospheres (Fig. 2A-C).

Alterations of the mNSC secretome during ZIKV infection.

Neural cells routinely secrete proteins involved in repair, restoration, and regeneration of injured brain tissue. Cytokines, chemokines, and growth factors are all secreted by neural cells in response to certain stimuli and can be regarded as the neural "secretome" (Drago et al., 2013; Skalnikova et al., 2011). We hypothesized that ZIKV infection alters the neural secretome and analysis of both uninfected and infected secretomes will allow us to create a model of ZIKV neuropathogenesis.

To determine if ZIKV alters the mNSCs secretome, mNSCs were inoculated with approximately 5 x 10^4 genomic equivalents of ZIKV, unbound virus was removed, and then fresh media was added to each infection. Mock-infected controls were included. mNSC media lacked serum but included basic fibroblast growth factor and epidermal growth factor. This meant that depletion of serum proteins was not needed for secretome analysis. Cell-free supernatants were then collected 1 and 7 dpi and submitted for liquid chromatography tandem mass spectrometry (LC+MS/MS). All MS/MS samples were analyzed using Mascot, and set up to search the NCBInr_20130403 database (selected for Mus, unknown version, 144,484 entries) assuming trypsin as the digestion enzyme. Mascot was searched with a fragment ion mass tolerance of 0.020 Da and a parent ion tolerance of 10.0 PPM. Carbamidomethyl of cysteine was specified in Mascot as a fixed modification. Gln->pyro-Glu of the n-terminus, deamidated of

asparagine and glutamine and oxidation of methionine were specified in Mascot as variable modifications.

Scaffold version 4.4.8 was used to validate MS/MS based peptide and protein identifications. Peptide identifications were accepted if they could be established at greater than 50.0% probability by the Peptide Prophet algorithm with Scaffold delta-mass correction. Protein identifications were accepted if they could be established at greater than 50.0% probability and contained at least 1 identified peptide. Protein probabilities were assigned by the Protein Prophet algorithm.

We identified a total of 22 and 68 proteins at 1 and 7 dpi, respectively (Fig. 3A-B). Interestingly only 12 proteins had signal peptides as predicted by SignalP 4.1, which suggested that proteins may be secreted or released from mNSCs independent from a traditional secretory pathway such as through non-specific shedding of surface proteins or co-packing into exocytic vesicles (Tables 1-4). Although unique proteins were present at both time points during ZIKV infection, neither of these proteins was present at both time points.

ZIKV-induced proteins 1 dpi include glia maturation factor-beta, glutamyl-prolyl-tRNA synthetase (EPRS), alpha-N-acetylglucosaminidase, mCG130239, and dopey family member 2, isoform CRA_a. Glia maturation factor-beta causes differentiation of brain cells and stimulates neural regeneration, glutamyl-prolyl-tRNA synthetase (EPRS) catalyzes aminoacylation of glutamic acid and proline tRNA species, alpha-N-acetylglucosaminidase breaks down glycosaminoglycans, mCG130239 is a cytochrome p450 family member, and dopey family

member 2, isoform CRA_a may be involved in protein traffic between late Golgi and early endosomes. Each of these proteins except for ERPS and mcG130239 has specific physiological roles in the brain (Table 1).

ZIKV-induced proteins at 7 dpi include mcG131554, isoform CRA_b, Mtf2 protein, ancient conserved domain protein 1, mCG128875, isoform CRA_a, mCG50378, mcG3623, isoform CRA_b, and carbohydrate sulfotransferase 9, isoform CRA_a. mcG131554, isoform CRA_b is a zinc-finger containing protein, Mtf2 protein is a member of the polycomb group of proteins and regulates transcriptional networks during embryonic self-renewal and differentiation, ancient conserved domain protein 1 is a putative metal transporter, mCG128875, isoform CRA_a contains a myosin-like motor domain, mCG50378 and mcG3623, isoform CRA_b are members of the L21-like ribosomal protein family, and carbohydrate sulfotransferase 9, isoform CRA_a modify extracellular carbohydrates for intercellular communication, cellular adhesion, and extracellular matrix maintenance (Table 2).

More striking is the larger number of proteins detected in mock-infected supernatants compared to ZIKV-infected supernatants at both time points. In particular, 52 proteins were detected in mock-infected supernatants and only 7 were detected in ZIKV-infected supernatants at 7 dpi. A number of proteins with specific physiological roles in brain development and function are absent in ZIKV-infected supernatants. Examples include guanylyl cyclase receptor, which is involved in NSC proliferation, synaptotagmin-like protein 2-b, which is a membrane-trafficking protein that mediates neural development and neurotransmission, and mesoderm differentiation and neurogenesis protein, which is involved in neural development (Tables 3-4).

Many other proteins involved in various cellular processes ranging from metabolism to formation of the extracellular matrix are also present in mock-infected supernatants but absent in ZIKV-infected supernatants.

ZIKV infection induces astrocyte differentiation genes and TLR3.

ZIKV led to marked CPE and changes in the mNSC secretome. Based on previous literature, we hypothesized that ZIKV would lead to apoptosis of infected cells and that extensive cell death would eliminate our cultured cells. To test this hypothesis, we infected mNSC for 7 days and then passaged cells into fresh media. Surprisingly, the resulting neurospheres did not exhibit CPE, yet still replicated ZIKV to similar titers as unpassaged mNSCs (Fig. 4A-B).

Previous literature suggested that specific neuronal lineages are specifically targeted by ZIKV (Li et al., 2016; Tang et al., 2016). To test this hypothesis, we performed a gene expression array on RNA extracted from mock and ZIKV-infected mNSC at 1 and 7 dpi. The array targeted a number of neural stem cell progenitor and differentiation markers, including genes that are associated with neural stem cells (nestin), neural precursors (Sox2, Pax6), neuron-restricted progenitors (DCX), neurons (Tuj1), differentiated postmitotic neurons (NeuN, synaptophysin), glutamatergic neurons (GAD65), serotonergic neurons (5-HTT), dopaminergic neurons (VMAT2, DAT), peripheral neurons (calretenin), oligodendrocytes (Mash1, GalC), astrocytes (GFAP, ALPH1a), and Schwann cells (MBP) (Table 5). The gene expression array suggested that mNSCs were comprised mostly of neuronal and oligodendrocyte progenitors at 1 dpi, although a markers of astrocyte differentiation were present at 7 dpi (Fig. 5A-B). ZIKV

infection led to dramatic changes in gene expression at both time points. Genes associated with neural precursors (Sox2), neurons (Tuj1), and differentiated postmitotic neurons (NeuN, synaptophysin) were downregulated, while genes associated with a neural stem cell marker (nestin), and neuron-restricted progenitors (DCX) were upregulated at 1 dpi (Figure 5A). Genes associated with neural stem cell marker (nestin), neural precursors (Sox2), neural-restricted progenitors (DCX), differentiated postmitotic neurons (synaptophysin), dopaminergic neurons (DAT), and oligodendrocytes (Mash1, GalC) were downregulated, while genes associated with peripheral neurons (calretenin) and astrocytes (GFAP, ALDH1a) were upregulated at 7 dpi (Fig. 5B). ALDH1a is a marker of astrocyte differentiation and had the highest fold-change in gene expression during ZIKV infection (Fig. 5C). We hypothesized that mNSCs induce astrocytes in order to initiate an innate immune response against ZIKV. Accordingly, we assessed the level of Toll-like receptor 3 (TLR3) expression in mock and ZIKV-infected mNSCs 1 and 7 dpi. mNSCs significantly upregulated TLR3 7 dpi (Fig. 5D). These data suggest that ZIKV alters differentiation of neural stem cells, neuronal cell types, and oligodendrocyte precursors, and induces differentiation of astrocytes, which correlates with an increase in TLR3 expression and a reduction in CPE.

ZIKV infection induces neuroprotective response in astrocytes differentiated from mouse neural stem cells

Our previous data indicated that ZIKV infection induced markers of astrocyte differentiation. TLR3 expression was also increased. We hypothesized that ZIKV infection leads to differentiation of astrocytes as an antiviral response. To test this hypothesis, we differentiated mNSCs into astrocytes and then inoculated cells with approximately 5 x 10^4 genomic equivalents ZIKV. Gene expression of a number of astrocyte-associated genes was assessed 7 dpi (Fig. 6).

The array consisted of genes associated with antiviral response (TLR3, viperin), inflammatory response (BAFF, CCL2, CXCL10, galectin-9, Il10), glial activation (Birc3, Gpr84), as well as neurotrophic factors (BDNF, VEGF). Infection with ZIKV upregulated TLR3 and viperin, both of which are involved in antiviral processes. ZIKV infection also upregulated CCL2, a chemokine involved in immunoregulatory and inflammatory pathways. ZIKV infection upregulated Gpr84, which is an astrocyte activation marker. Brain-derived neurotropic factor (BDNF) and vascular endothelial growth factor (VEGF), two neurotrophic factors involved in neurogenesis and tissue repair, were also upregulated following ZIKV infection.

Discussion

The scientific community has responded rapidly to the current ZIKV outbreak. Multiple *in vitro* and *in vivo* models have already been reported that show ZIKV neurotropism and negative effects on neural cell growth, survival, and differentiation (Aliota et al., 2016; Dowall et al., 2016; Garcez et al., 2016; Lazear et al., 2016; Li et al., 2016; Tang et al., 2016). We expanded on this work by assessing the impact of ZIKV infection on the secreted proteome and differentiation of neural stem cells.

ZIKV infection led to clear CPE in mNSCs, which persisted throughout a 7 day time course. This was associated with a significant decrease in the number of proteins detected in cell free supernatants. This decrease in protein number may be due to the decrease in neurospheres in ZIKV-infected wells, although it is unlikely that the less than 2-fold decrease in neurospheres accounted for the 8-fold decrease in proteins that were identified. We also noted the presence of a number of unique proteins during ZIKV infection. These proteins appear to be classified as

reparative, proviral, and antiviral components. For example, glia maturation factor-beta causes differentiation of brain cells and stimulates neural regeneration. We hypothesize that glia maturation factor-beta is secreted by infected cells to protect against neurological damage by inducing differentiation of astrocytes. This is supported by our gene expression array data showing upregulation of GFAP, ALDH1a, and associated antiviral and inflammatory genes. Mtf2 is also involved in neural regeneration and may also protect against neurological damage. The protein alpha-N-acetylglucosaminidase breaks down glycosaminoglycans, which prevent flavivirus dissemination and neurovirulence *in vivo*. We hypothesize that alpha-N-acetylglucosaminidase may enhance ZIKV dissemination in the brain. Dopey family member 2, isoform CRA_a may be involved in protein traffic between late Golgi and early endosomes, which is a likely pathway used by ZIKV to secrete progeny into the extracellular environment. mCG128875, isoform CRA_a contains a myosin-like motor domain, which may also be involved in ZIKV secretion. mcG131554, isoform CRA_b is a zinc-finger containing protein, which may represent an antiviral protein that binds to viral RNA.

It is important to note that not all neurospheres were disaggregated during ZIKV infection. Fifty percent of neurospheres were morphologically normal at 4 dpi. Upon passage of ZIKV-infected mNSCs at 7 dpi, all neurospheres were morphologically normal and there was no evidence of CPE. Our gene expression array confirmed that ZIKV led to dramatic changes in the expression of genes associated with neural stem cell differentiation. Most genes expressed in mNSCs were downregulated upon ZIKV infection; however, both astrocyte differentiation markers (GFAP, ALDH1a) and TLR3 were significantly upregulated at 7 dpi. Astrocytes play major roles in inflammatory and immune responses during viral infection and express Toll-like

receptors crucial for the induction of innate immune responses in the central nervous system through detection of virus-derived dsRNA (Lafaille et al., 2012; Liu et al., 2013; Nocon et al., 2014). We hypothesize that induction of astrocyte differentiation and TLR3 was a neuroprotective response that reduced CPE in our model, although it is clear that reactive astrocytosis can both protect and lead to neuropathogenesis *in vivo*.

Our gene expression data on astrocytes differentiated from mNSCs provides support that ZIKV infection induces an antiviral response that can be neuroprotective. We confirmed astrocyte reactivity by showing an upregulation of Gpr84, a protein indicating astrocyte activation, and, like the mNSCs, these astrocytes also induced a TLR3 response that is believed to protect against viral neuropathogenesis. Accordingly, the infected astrocytes also upregulated expression of viperin, a protein that participates in the antiviral response produced by TLR3 activation (Rivieccio et al., 2006). We hypothesize that viperin is produced by infected cells to deter further infection, as it functions to inhibit viral replication by attacking vital structural components of viruses, including flaviviruses such as West Nile and Dengue (Helbig and Beard, 2014; Jiang et al., 2010; Wang et al., 2015). Upregulation of BDNF and VEGF by the astrocytes increases evidence of a neuroprotective response. Both of these neurotrophic factors are involved in neurogenesis and neurogeneration, and seem to be produced to facilitate a protective response, presumably through TLR3 activation, as activation of this toll-like receptor is associated with release of various neuroprotective factors (Bsibsi et al., 2006).

In summary, our data indicate that ZIKV productively infects mNSCs and leads to CPE and alterations in the secreted proteome. We detected proteins that were only secreted during

ZIKV infection such as proteins responsible for repair or neurological damage, and proteins that promote and antagonize viral infection. We hypothesized that the above cytological and proteomic alterations may prevent differentiation of neural cell types. Accordingly, we found that ZIKV infection significantly reduced gene expression of markers associated with neuronal and oligodendrocyte progenitors, while increasing gene expression of markers associated with astrocyte progenitors – a cell type associated with mediating the innate immune response against virus infection. We confirmed a protective immune response after finding that astrocyte differentiated from mNSCs upregulated expression of various antiviral and neuroprotective genes. A major caveat to this study is the use of the ZIKV IB H strain, which is from the African lineage and has not been previously associated with congenital ZIKV syndrome. Additionally, ZIKV IB H strain was extensively passaged in mouse brains, which may have selected mutations that alter its behavior in neural cells and tissues. *In vivo* models are necessary to determine which ZIKV strains can most accurately recapitulate human disease.

Materials and Methods

Virus and cell culture.

African lineage Zika virus (ZIKV) strain IB H 30656 was obtained from ATCC and passaged in C6/36 cells one time prior to these experiments. Cells were inoculated with 5 x 10^4 genomic equivalents of ZIKV. C6/36 cells were maintained in DMEM containing 10% fetal bovine serum, tryptose phosphate, and antibiotics at 30°C. To collect mouse neural stem cells (mNSCs), the cortical layer was dissected from embryonic day 14 (E14) mice and manually dissociated. After the removal of debris, cells were collected following centrifugation, and maintained in NSC proliferation medium consisting of DMEM/F-12, L-alanyl-L-glutamine, B-

27 (minus vitamin A), N-2 supplement, basic fibroblast growth factor (bFGF), epidermal growth factor (EGF), and penicillin-streptomycin at 37°C with 5% CO_2. To differentiate mNSCs to astrocyte, the cells were plated on to poly-l-lysine-coated coverslips and maintained in NSC proliferation medium at 37°C with 5% CO_2 for two days. The cells were then maintained in astrocyte differentiation medium consisting of DMEM, N-2 supplement, L-alanyl-L-glutamine, fetal bovine serum (FBS), and penicillin-streptomycin at 37°C with 5% CO_2 for 14 days, to allow the cells to differentiate to astrocytes.

Ethics statement.

Animals were maintained and procedures were performed in accordance with the recommendations in the Guide for the Care and Use of Laboratory Animals of the National Research Council. Proposal YAC128, R6/2, 5xFAD was approved by the Central Michigan University IACUC committee. Approved euthanasia criteria were based on weight loss and morbidity.

qRT-PCR-based infectivity assay.

mNSCs were seeded at approximately 20,000 cells/well in 96-well plates and then 5 x 10^4 genomic equivalents of ZIKV was inoculated to cells in a total volume of 100 µL for 1 hr. at 37°C. Unbound virus was then removed, and fresh media was added. mNSCs were gently centrifuged between each step to prevent cell loss. Samples were taken at this time point and set as day 0. Plates were then gently tapped to prevent neurospheres from adhering to the cell culture plates, which would promote differentiation. Infections progressed for up to 7 days, and samples were taken on 1, 3, 5, and 7 days post-infection. For analysis of relative viral vRNA, total mRNA

was harvested using RNeasy kits from 10 µL of cell free supernatants (Qiagen). Reverse transcription and quantitative PCR were performed in the same closed tube with 100 ng of total RNA per reaction using the Quantitect RT-PCR Kit (Qiagen) on an Eco Real-Time PCR System (Illumina) with a total reaction volume of 10 µl. Cycling conditions were 50°C for 30 min (reverse transcription) and 95 °C for 15 min, followed by 45 cycles of 94 °C for 15 s, 55 °C for 30 s and 72 °C for 30 s. Relative quantities of target cDNA were determined using the Pfaffl method and a single data point from day 0 was set to 1.0 for each experiment.

Liquid chromatography tandem mass spectrometry.

Cell free supernatants were taken from mock and ZIKV-infected mNSCs at 1 and 7 dpi and submitted to the Interdisciplinary Center for Biotechnology Research at the University of Florida for liquid chromatography tandem mass spectrometry (LC+MS/MS). Charge state deconvolution and deisotoping were not performed. All MS/MS samples were analyzed using Mascot. Mascot was set up to search the NCBInr_20130403 database (selected for Mus., unknown version, 144484 entries) assuming the digestion enzyme trypsin. Mascot was searched with a fragment ion mass tolerance of 0.020 Da and a parent ion tolerance of 10.0 PPM. Carbamidomethyl of cysteine was specified in Mascot as a fixed modification. Gln->pyro-Glu of the n-terminus, deamidated of asparagine and glutamine and oxidation of methionine were specified in Mascot as variable modifications. Scaffold (version Scaffold_4.4.8, Proteome Software Inc., Portland, OR) was used to validate MS/MS based peptide and protein identifications. Peptide identifications were accepted if they could be established at greater than 50.0% probability by the Peptide Prophet algorithm with Scaffold delta-mass correction. Protein identifications were accepted if they could be established at greater than 50.0% probability and

contained at least 1 identified peptide. Protein probabilities were assigned by the Protein Prophet algorithm.

qRT-PCR gene expression array.

To determine the lineage of mNSCs following ZIKV infection, qRT-PCR was performed to determine relative gene expression of various neural stem cell progenitor and differentiation markers. To determine immune response of astrocytes differentiated from mNSCs following ZIKV infection, qRT-PCR was performed to determine relative gene expression of various inflammatory, glial, and neurotrophic genes. Total RNA from mock- and ZIKV-infected cells was extracted 1 and 7 dpi using the RNeasy kit (Qiagen). cDNA synthesis was performed using the High Capacity RNA-to-cDNA Kit (Applied Biosystems) on a DNA Engine Dyad Thermal Cycler (MJ Research). Quantitative PCR (qPCR) was performed in triplicate on a StepOnePlus Real-Time PCR System (Applied Biosystems) using SYBR Green PCR Master Mix (Applied Biosystems) in a total reaction volume of 20 μL. Cycling conditions were as specified by the manufacturer. Gene targets and their respective sequences are listed in Table 5. Gene expression was normalized to the GAPDH reference gene and nestin gene expression in mock-infected cells 1 dpi was set to 1.0.

Acknowledgements

We thank Tonya Colpitts at the University of South Carolina School of Medicine for helping our team develop the experimental aims for this project.

References

Aliota, M.T., Caine, E.A., Walker, E.C., Larkin, K.E., Camacho, E., Osorio, J.E., 2016. Characterization of Lethal Zika Virus Infection in AG129 Mice. PLoS Negl Trop Dis 10, e0004682.

Bell, T.M., Field, E.J., Narang, H.K., 1971. Zika virus infection of the central nervous system of mice. Arch Gesamte Virusforsch 35, 183-193.

Belzile, J.P., Stark, T.J., Yeo, G.W., Spector, D.H., 2014. Human cytomegalovirus infection of human embryonic stem cell-derived primitive neural stem cells is restricted at several steps but leads to the persistence of viral DNA. J Virol 88, 4021-4039.

Bsibsi, M., Persoon-Deen, C., Verwer, R.W.H., Meeuwsen, S., Ravid, R., Van Noort, J.M., 2006. Toll-like Receptor 3 on Adult Human Astrocytes Triggers Production of Neuroprotective Mediators. Glia 53, 688-695.

Calvet, G., Aguiar, R.S., Melo, A.S., Sampaio, S.A., de Filippis, I., Fabri, A., Araujo, E.S., de Sequeira, P.C., de Mendonca, M.C., de Oliveira, L., Tschoeke, D.A., Schrago, C.G., Thompson, F.L., Brasil, P., Dos Santos, F.B., Nogueira, R.M., Tanuri, A., de Filippis, A.M., 2016. Detection and sequencing of Zika virus from amniotic fluid of fetuses with microcephaly in Brazil: a case study. Lancet Infect Dis 16, 653-660.

Dowall, S.D., Graham, V.A., Rayner, E., Atkinson, B., Hall, G., Watson, R.J., Bosworth, A., Bonney, L.C., Kitchen, S., Hewson, R., 2016. A Susceptible Mouse Model for Zika Virus Infection. PLoS Negl Trop Dis 10, e0004658.

Drago, D., Cossetti, C., Iraci, N., Gaude, E., Musco, G., Bachi, A., Pluchino, S., 2013. The stem cell secretome and its role in brain repair. Biochimie 95, 2271-2285.

Fauci, A.S., Morens, D.M., 2016. Zika Virus in the Americas - Yet Another Arbovirus Threat. N Engl J Med 374, 601-604.

Garcez, P.P., Loiola, E.C., Madeiro da Costa, R., Higa, L.M., Trindade, P., Delvecchio, R., Nascimento, J.M., Brindeiro, R., Tanuri, A., Rehen, S.K., 2016. Zika virus impairs growth in human neurospheres and brain organoids. Science 352, 816-818.

Grard, G., Caron, M., Mombo, I.M., Nkoghe, D., Mboui Ondo, S., Jiolle, D., Fontenille, D., Paupy, C., Leroy, E.M., 2014. Zika virus in Gabon (Central Africa)--2007: a new threat from Aedes albopictus? PLoS Negl Trop Dis 8, e2681.

Helbig, K.J., Beard, M.R., 2014. The Role of Viperin in the Innate Antiviral Response. J Mol Bio 426, 1210-1219.

Jiang, D., Weidner, J.M., Qing, M., Pan, X.B., Guo, H., Xu, C., Zhang, X., Birk, A., Chang, J., Shi, P.Y., Block, T.M., Guo, J.T., 2010. Identification of Five Interferon-Induced Cellular Proteins That Inhibit West Nile Virus and Dengue Virus Infections. J Virol 84, 8332-8341.

Kosugi, I., Shinmura, Y., Li, R.Y., Aiba-Masago, S., Baba, S., Miura, K., Tsutsui, Y., 1998. Murine cytomegalovirus induces apoptosis in non-infected cells of the developing mouse brain and blocks apoptosis in primary neuronal culture. Acta Neuropathol 96, 239-247.

Lafaille, F.G., Pessach, I.M., Zhang, S.Y., Ciancanelli, M.J., Herman, M., Abhyankar, A., Ying, S.W., Keros, S., Goldstein, P.A., Mostoslavsky, G., Ordovas-Montanes, J., Jouanguy, E., Plancoulaine, S., Tu, E., Elkabetz, Y., Al-Muhsen, S., Tardieu, M., Schlaeger, T.M., Daley, G.Q., Abel, L., Casanova, J.L., Studer, L., Notarangelo, L.D., 2012. Impaired intrinsic immunity to HSV-1 in human iPSC-derived TLR3-deficient CNS cells. Nature 491, 769-773.

Lazear, H.M., Govero, J., Smith, A.M., Platt, D.J., Fernandez, E., Miner, J.J., Diamond, M.S., 2016. A Mouse Model of Zika Virus Pathogenesis. Cell Host Microbe 19, 720-730.

Li, C., Xu, D., Ye, Q., Hong, S., Jiang, Y., Liu, X., Zhang, N., Shi, L., Qin, C.F., Xu, Z., 2016. Zika Virus Disrupts Neural Progenitor Development and Leads to Microcephaly in Mice. Cell Stem Cell 19, 120-126.
Li, X.J., Liu, X.J., Yang, B., Fu, Y.R., Zhao, F., Shen, Z.Z., Miao, L.F., Rayner, S., Chavanas, S., Zhu, H., Britt, W.J., Tang, Q., McVoy, M.A., Luo, M.H., 2015. Human Cytomegalovirus Infection Dysregulates the Localization and Stability of NICD1 and Jag1 in Neural Progenitor Cells. J Virol 89, 6792-6804.
Liu, Z., Guan, Y., Sun, X., Shi, L., Liang, R., Lv, X., Xin, W., 2013. HSV-1 activates NF-kappaB in mouse astrocytes and increases TNF-alpha and IL-6 expression via Toll-like receptor 3. Neurol Res 35, 755-762.
Martines, R.B., Bhatnagar, J., Keating, M.K., Silva-Flannery, L., Muehlenbachs, A., Gary, J., Goldsmith, C., Hale, G., Ritter, J., Rollin, D., Shieh, W.J., Luz, K.G., Ramos, A.M., Davi, H.P., Kleber de Oliveria, W., Lanciotti, R., Lambert, A., Zaki, S., 2016. Notes from the Field: Evidence of Zika Virus Infection in Brain and Placental Tissues from Two Congenitally Infected Newborns and Two Fetal Losses - Brazil, 2015. MMWR Morb Mortal Wkly Rep 65, 159-160.
Nocon, A.L., Ip, J.P., Terry, R., Lim, S.L., Getts, D.R., Muller, M., Hofer, M.J., King, N.J., Campbell, I.L., 2014. The bacteriostatic protein lipocalin 2 is induced in the central nervous system of mice with west Nile virus encephalitis. J Virol 88, 679-689.
Rivieccio, M.A., Suh H.S., Zhao, Y., Zhao, M.L., Chin K.C., Lee, S.C., Brosnan, C.F., 2006. TLR3 Ligation Activates an Antiviral Response in Human Fetal Astrocytes: A Role for Viperin/cig5. J Immuno 177, 4735-4741.
Rossi, S.L., Tesh, R.B., Azar, S.R., Muruato, A.E., Hanley, K.A., Auguste, A.J., Langsjoen, R.M., Paessler, S., Vasilakis, N., Weaver, S.C., 2016. Characterization of a Novel Murine Model to Study Zika Virus. Am J Trop Med Hyg 94, 1362-1369.
Skalnikova, H., Motlik, J., Gadher, S.J., Kovarova, H., 2011. Mapping of the secretome of primary isolates of mammalian cells, stem cells and derived cell lines. Proteomics 11, 691-708.
Tang, H., Hammack, C., Ogden, S.C., Wen, Z., Qian, X., Li, Y., Yao, B., Shin, J., Zhang, F., Lee, E.M., Christian, K.M., Didier, R.A., Jin, P., Song, H., Ming, G.-l., 2016. Zika Virus Infects Human Cortical Neural Progenitors and Attenuates Their Growth. Cell Stem Cell 18, 587-590.
Tsutsui, Y., Kosugi, I., Kawasaki, H., Arai, Y., Han, G.P., Li, L., Kaneta, M., 2008. Roles of neural stem progenitor cells in cytomegalovirus infection of the brain in mouse models. Pathol Int 58, 257-267.
Wong, P.S., Li, M.Z., Chong, C.S., Ng, L.C., Tan, C.H., 2013. Aedes (Stegomyia) albopictus (Skuse): a potential vector of Zika virus in Singapore. PLoS Negl Trop Dis 7, e2348.
Wang, B., Fang, Y., Wu, Y., Koga, K., Osuga, Y., Lv, S., Chen, D., Zhu, Y., Wang, J., Huang, H., 2015. Viperin is induced following toll-like receptor 3 (TLR3) ligation and has a virus-responsive function in human trophoblast cells. Placenta 36, 667-673.

Figure Legends

Figure 1

Infection of mNSCs with ZIKV. Mouse neural stem cells (mNSCs) were inoculated with ZIKV. Unbound virus was removed after one hour and fresh media was added to each infection. Cell free supernatants were collected at this time and set as day 0 (D0). Cell free supernatants were then collected 1, 3, 5, and 7 days post-infection (dpi) (D1, D3, D5, and D7). RNA was extracted each from cell free supernatants and qRT-PCR was performed on three independent samples and normalized to µL of supernatant.

Figure 2

ZIKV infection of mNSCs reduces neurosphere numbers and induces cytopathic effect. Mouse neural stem cells (mNSCs) were inoculated with ZIKV. Unbound virus was removed after one hour and fresh media was added to each infection. (A) The number of neurospheres were counted in mock and ZIKV-infected wells at 10X magnification 3 and 5 dpi. (B) Duplicate representative images of neurospheres in mock and ZIKV-infected wells at 20X magnification 5 dpi. (C) Duplicate representative images of neurospheres in mock and ZIKV-infected wells at 40X magnification 5 dpi.

Figure 3

Venn diagrams of LC+MS/MS data. (A) Number of unique and common proteins detected in mock and ZIKV-infected cell free mouse neural stem cell (mNSC) supernatants 1 dpi. (B) Number of unique and common proteins detected in mock and ZIKV-infected cell free mNSC supernatants 7 dpi.

Figure 4

Replication of ZIKV in passaged mNSCs. (A) Unpassaged mouse neural stem cells (mNSCs) (P0) were inoculated with ZIKV. Unbound virus was removed after one hour and fresh media was added to each infection. Cell free supernatants were then collected 1, 3, and 5 days post-infection (dpi) (D1, D3, and D5). Infections progressed for 7 days and then mNSCs were passaged into fresh media. Cell free supernatants were then collected at 1, 3, and 5 dpi from the passaged cells (P1). RNA was extracted each from cell free supernatants and qRT-PCR was performed on three independent samples and normalized to µL of supernatant. (B) Representative image of passaged neurospheres ZIKV-infected wells at 20X magnification at 5 dpi.

Figure 5

qRT-PCR gene expression array of neural stem cell progenitors and differentiation markers during ZIKV infection of mNSCs. Mouse neural stem cells (mNSCs) were mock or ZIKV-infected and total cellular RNA was extracted at (A) 1 and (B) 7 days post-infection (dpi). RNA was converted to cDNA and a panel of genes representing neural stem cell progenitors and differentiation markers were amplified. (C) Relative expression of ALDH1a in mock and ZIKV-infected mNSCs at 7 dpi. (D) Relative expression of TLR3 in mock and ZIKV-infected mNSCs at 1 and 7 dpi. qRT-PCR was performed on three independent samples and normalized to GAPDH. Nestin gene expression in mock-infected cells at 1 dpi was set to 1.0. Mock (black) and ZIKV-infected (gray) samples are grouped together for each gene. Student's t tests were performed to assess statistical significance between groups. * $p<0.001$; ŧ $p<0.01$

Figure 6

qRT-PCR gene expression array of astrocytes differentiated from mouse neural stem cells. Astrocytes differentiated from mouse neural stem cells (mNSCs) were mock or ZIKV-infected and total cellular RNA was extracted 7 days post-infection (dpi). RNA was converted to cDNA and a panel of genes associated with the antiviral response, inflammation, glial activation, and neurotrophic factors were amplified. qRT-PCR was performed on three independent samples and normalized to GAPDH. Toll-like receptor 3 (TLR3) gene expression in mock-infected cells was set to 1.0. Mock (black) and ZIKV-infected (gray) samples are grouped together for each gene. Student's t tests were performed to assess statistical significance between groups. * $p<0.001$

Table 1. LC+MS/MS hits specific to ZIKV-infected mNSC cell supernatant 1 dpi

Identifier	Comment	SignalP
gi|10764635	glia maturation factor-beta	No
gi|148681120	glutamyl-prolyl-tRNA synthetase	No
gi|254910995	alpha-N-acetylglucosaminidase precursor	Yes
gi|148709876	mCG130239	Yes
gi|148671813	dopey family member 2, isoform CRA_a	No

Table 2. LC+MS/MS hits specific to ZIKV-infected mNSC cell supernatant 7 dpi

Identifier	Comment	SignalP
gi|148707695	mCG131554, isoform CRA_b	No
gi|116283410	Mtf2 protein	No
gi|121955985	ancient conserved domain protein 1	No
gi|148669275	mCG128875, isoform CRA_a	No
gi|148683831	mCG50378	No
gi|148687012	mCG3623, isoform CRA_b	No
gi|148669657	carbohydrate sulfotransferase 9, isoform CRA_a	No

Table 3. LC+MS/MS hits specific to mock-infected mNSC cell supernatant 1 dpi

Identifier	Comment	SignalP
gi|163310765	serum albumin precursor	Yes
gi|148695014	lymphocyte antigen 75	Yes
gi|13878227	WD repeat-containing protein 6	No
gi|1196535	guanylyl cyclase receptor	No
gi|124487125	K/Na hyperpolarization-activated cyclic nucleotide-gated channel 4	No
gi|19343974	Slc16a4 protein	No
gi|148699105	jumonji domain containing 2C, isoform CRA_b	No
gi|1212744	a1(XI) collagen chain	No
gi|124486951	protein polybromo-1	No
gi|26344399	unnamed protein product	No
gi|109734516	Zinc finger protein 287	No
gi|6678509	uricase	No

Table 4. LC+MS/MS hits specific to mock-infected mNSC cell supernatant 7 dpi

Identifier	Comment	SignalP
gi|12841072	unnamed protein product	No
gi|221237024	Fv1 gammaretrovirus restriction factor	No
gi|163310765	serum albumin precursor	Yes
gi|147905039	protein QN1 homolog	No
gi|1196535	guanylyl cyclase receptor	No
gi|1587060	alpha dystroglycan	Yes
gi|124487125	K/Na hyperpolarization-activated cyclic nucleotide-gated channel 4	No
gi|19343974	Slc16a4 protein	No
gi|12859995	unnamed protein product	No
gi|407261488	zinc finger protein 729-like	No
gi|1235676	metalloprotease/disintegrin/cysteine rich protein precursor	Yes
gi|13543830	Usp52 protein, partial	No
gi|148670574	mCG1040741, isoform CRA_b	No
gi|148675448	src-related kinase	No
gi|148704364	mCG142372	No
gi|60360376	mKIAA1195 protein	No
gi|294610675	beta-galactosidase-like protein precursor	Yes
gi|1203899	G protein-coupled receptor Rec1.3	No
gi|118136302	fibrillin-2 precursor	Yes
gi|148693710	RIKEN cDNA D130054N24, isoform CRA_a	No
gi|14250365	Similar to RIKEN cDNA 4930527D15 gene, partial	No
gi|148686455	DEAH (Asp-Glu-Ala-His) box polypeptide 29, isoform CRA_a	No
gi|148671767	mCG147087	No
gi|148673927	relaxin/insulin-like family peptide receptor 2	Yes
gi|379318641	Structure Of Mouse Orc1 Bah Domain Bound To H4k20me2	No
gi|11036456	Nulp1	No
gi|12854313	unnamed protein product	No
gi|255003750	Transmembrane protein 88	No
gi|32449717	A230067G21Rik protein	No
gi|148693354	septin 7, isoform CRA_b	No
gi|309266718	PREDICTED: complement C3-like, partial	No
gi|148677025	mCG140503	No
gi|31982322	platelet glycoprotein V precursor	Yes
gi|11385416	striated muscle-specific serine/threonine protein kinase	No
gi|13647015	synaptotagmin-like protein 2-b	No
gi|148664713	mCG121979, isoform CRA_a	No
gi|148692356	Rho guanine nucleotide exchange factor (GEF) 1, isoform CRA_b	No
gi|159031211	putative oligoadenylate synthetase 1b	No
gi|8248965	mesoderm differentiation and neurogenesis protein	No
gi|126157475	kelch-like protein 34	No
gi|26364838	unnamed protein product	No
gi|7304991	cytochrome P450, family 2, subfamily g, polypeptide 1 precursor	Yes

gi|148699674	WD repeat domain 18, isoform CRA_b	No
gi|12006108	IRA1	No
gi|74186894	unnamed protein product	No
gi|12850252	unnamed protein product	No
gi|116292744	ATP-binding cassette sub-family A member 13	No
gi|148708022	mCG133041	No
gi|148704362	mCG133735	No
gi|12858539	unnamed protein product	No
gi|116812904	metabotropic glutamate receptor 8 precursor	No
gi|187954335	4921517L17Rik protein	No

Table 5. Primers used for qRT-PCR array

Gene Name	Forward	Reverse
Nestin	GAGGTGGCTACATACAGGACTC	AAGAGAAGCCTGGGAACCTC
Sox2	AACGCAAAAACCGTGATGCC	TTGAGAACTCCCTGCGAAGC
Pax6	CACCAGACTCACCTGACACC	TACGGGGCTCTGAGAACTGG
DCX	CGACCAAGACGCAAATGGAAC	CTTGTGCTTCCGCAGACTTC
Tuj1	TAGACCCCAGCGGCAACTAT	GTTCCAGGTTCCAAGTCCACC
NeuN	GGCAATGGTGGGACTCAAAA	GGGACCCGCTCCTTCAAC
Synaptophysin	GCAGTGGGTCTTTGCCATCTTC	GCACTCTCCGTCTTGTTGGC
GAD65	GGGGCTTTTGATCCTCTCTTG	AGTTGGCCCTCTCTACTCC
5-HTT	GACATCAGGAGGGGCGTATG	CCCAGCATTTCCTTCACGTC
VMAT2	CAGGGAATTGGCTCCTCCTG	GGGTCCCACTAAGACTCCCA
DAT	CCTCCATTAACTCCCTGACAAG	CATTGTGCTTCTGTGCCATG
Calretinin	AGATCCTGCCGACCGAAGAG	TTCCGCCAAGCCTCCATAAAC
Mash1	CCTACGACCCCCTTAGTCCA	TGCCATCCTGCTTCCAAAGT
GalC	AACCCTCGCACATGCACTAT	TGACCATGGCAACCCCATAA
GFAP	GAGTACCAGGACCTGCTCAA	TTCACCACGATGTTCCTCTT
ALDH1a	GAGGCCATCAATGGTGGGAA	TGAAAATGTCTCCATCACTCGGT
MBP	GTACCCTGGCTAAAGCAGAGC	GTAGTTCTCGTGTGTGAGTCCTTG
TLR3	GCTCTGGAAACACGCAAAC	AAGGATGTGGAGGTGAGACAG
Galectin-9	AAGGGGCGCAAACAGAAAACTC	ACATCTGTCCAGGGGTGCTG
Viperin	TCAAAAGCTGAGGAGGTGGTG	TAGGAGGCACTGGAAAACCTTC
BAFF	AGCTACCGAGGTTCAGCAAC	GCCGGTGTCAGGAGTTTGAC
CCL2	AGCCAACTCTCACTGAAGCC	GGGGCGTTAACTGCATCTGG
IL10	TGAATTCCCTGGGTGAGAAGC	ATCACTCTTCACCTGCTCCAC
CXCL10	TGGCATTCAAGGAGTACCTCTC	CGTGGACAAAATTGGCTTGC
Birc3	GGGGACGATTTAAAGGTATCGC	CTGATACCGCAGCCCACTTC
Gpr84	GACTGCCCCTCAAAAGACCTG	ACATGATGGAGACTGAGGTTCCC
VEGF	GAGGATGTCCTCACTCGGATG	GTCGTGTTTCTGGAAGTGAGCAA
BDNF	GAAGAGCTGCTGGATGAGGAC	TTCAGTTGGCCTTTTGATACC
GAPDH	TCAACAGCAACTCCCACTCTTCCA	ACCCTGTTGCTGTAGCCGTATTCA

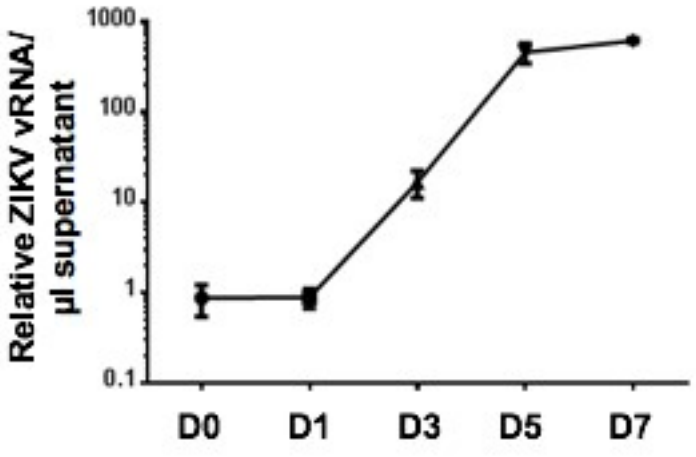
Relative ZIKV vRNA/
µl supernatant
1000
100
10
1
0.1
D0
D1
D3
D5
D7

Figure 1.

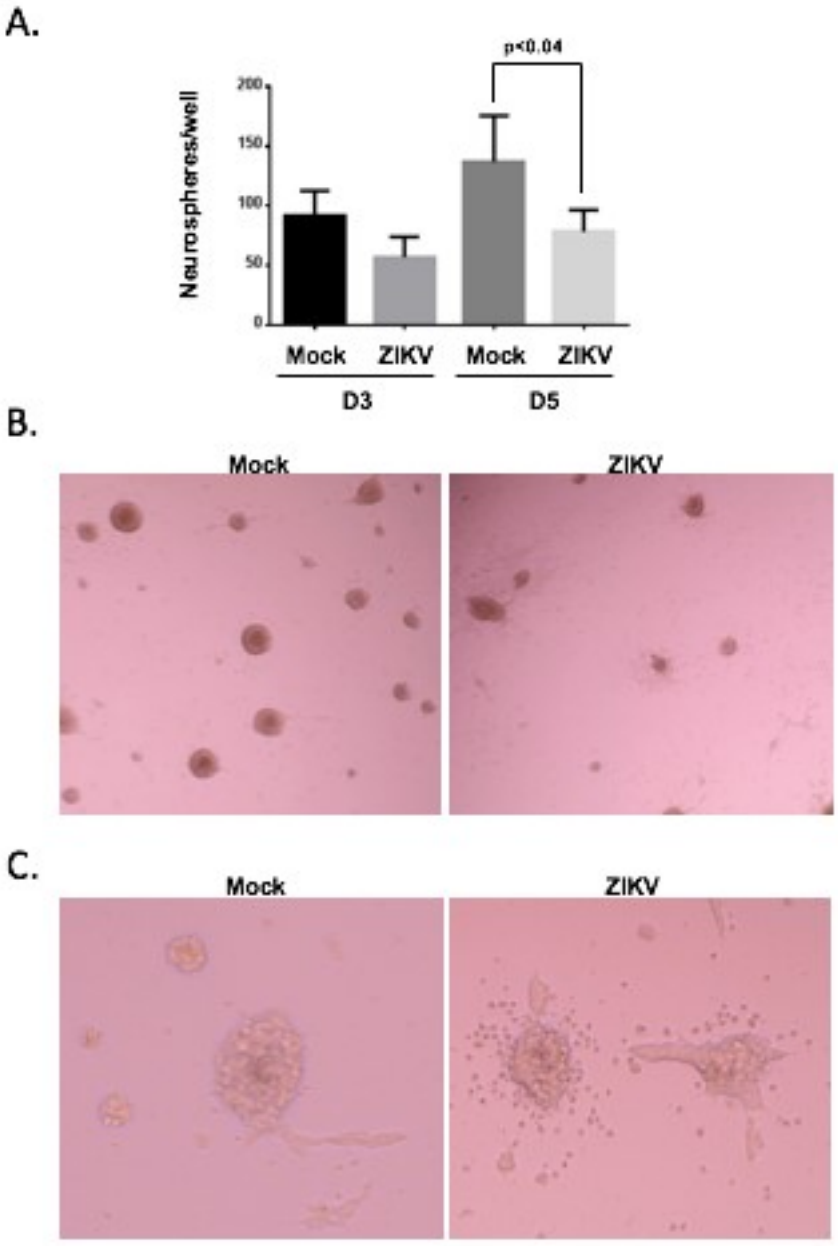
A.
p<0.04
Neurospheres/well
200
150
100
50
0
Mock
ZIKV
Mock
ZIKV
D3
D5
B.
Mock
ZIKV
C.
Mock
ZIKV

Figure 2.

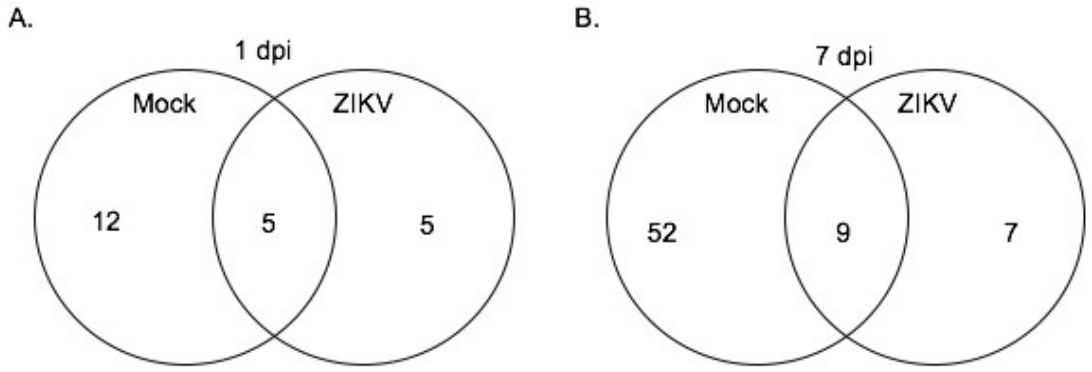

Figure 3.

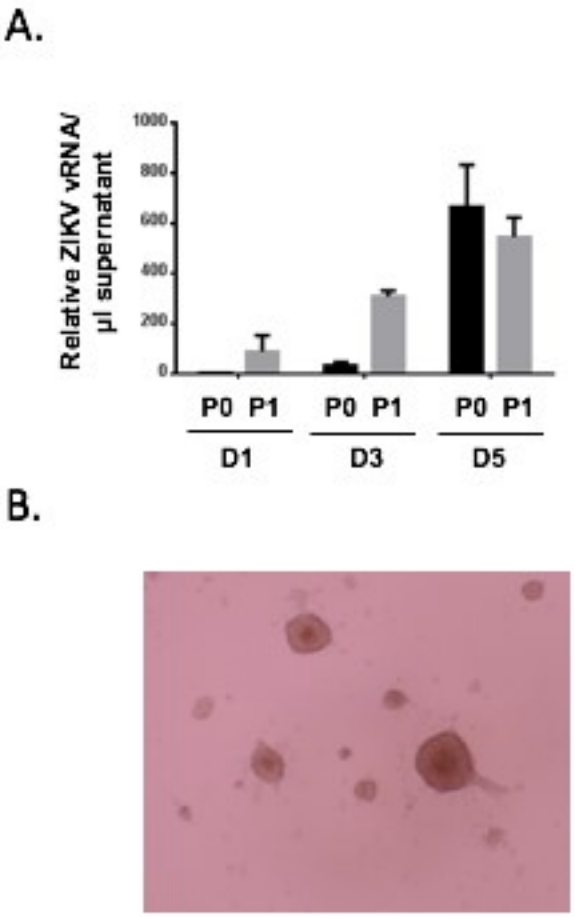

Figure 4.

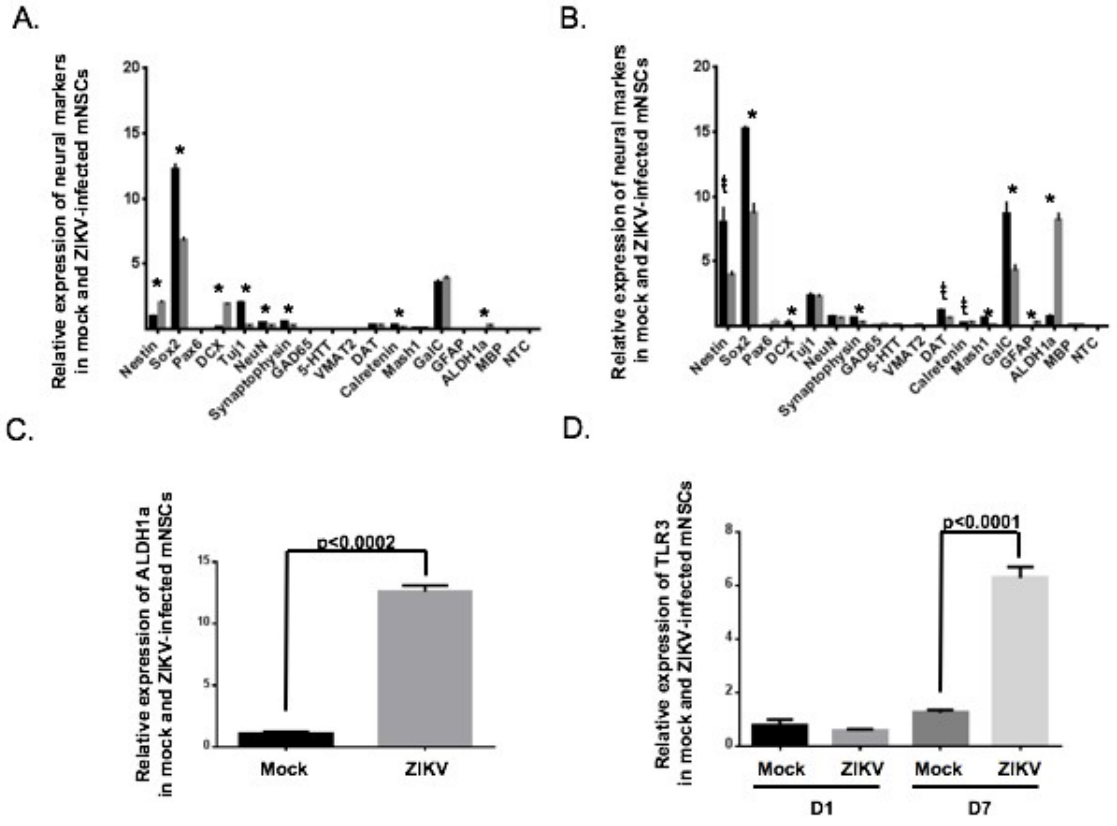
A.
B.
C.
D.
Relative expression of neural markers in mock and ZIKV-infected mNSCs
Nestin
Sox2
Pax6
DCX
Tuj1
NeuN
Synaptophysin
GAD65
5-HTT
VMAT2
DAT
Calretenin
Mash1
GalC
GFAP
ALDH1a
MBP
NTC
Relative expression of ALDH1a in mock and ZIKV-infected mNSCs
p<0.0002
Mock
ZIKV
Relative expression of TLR3 in mock and ZIKV-infected mNSCs
p<0.0001
Mock
ZIKV
Mock
ZIKV
D1
D7

Figure 5.

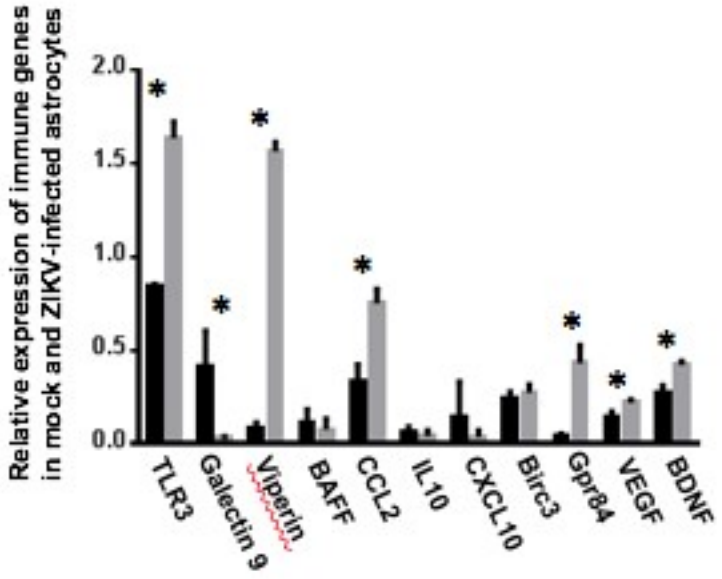
Relative expression of immune genes in mock and ZIKV-infected astrocytes
2.0
1.5
1.0
0.5
0.0
*
TLR3
Galectin 9
Viperin
BAFF
CCL2
IL10
CXCL10
Birc3
Gpr84
VEGF
BDNF

Figure 6.